

GENERATION OF KNOT NET FOR CALCULATION OF QUADRATIC TRIANGULAR B-SPLINE SURFACE OF HUMAN HEAD

Ján MIHALÍK *

This paper deals with calculation of the quadratic triangular B-spline surface of the human head for the purpose of its modeling in the standard videocodec MPEG-4 SNHC. In connection with this we propose an algorithm of generation of the knot net and present the results of its application for triangulation of the 3D polygonal model Candide. Then for the model and generated knot net as well as an established distribution of control points we show the results of the calculated quadratic triangular B-spline surface of the human head including its textured version for the texture of the selected avatar.

Key words: triangular B-spline, quadratic surface, knot net, human head, 3D polygonal model

1 INTRODUCTION

SNHC (Synthetic Natural Hybrid Coding) [1] is a subgroup of MPEG-4 [2] specialized in coding of graphical models of real or virtual three dimensional (3D) objects. Standardization of the coding extends the range of initial applications of MPEG-4 because it enables a combination of real and synthetic objects in the virtual environment. A very important 3D object in real and in virtual environment is the human head. SNHC introduces new algorithms of coding of the human head based on modeling its surface [3], animation [4] and texturing [5].

Analysis and synthesis of the human head in the videocodec MPEG-4 SNHC uses its polygonal (wire-frame) 3D models from the computer graphics. The models are, however, a course approximation of the human head surface, but by using suitable techniques of modeling [6] they one can be done more precisely with a very good smoothness. Recently, the area of graphical modeling is always a subject of research interest, especially from the point of view of new construction methods of 3D objects. First, in the paper, we describe and present a procedure of calculation the quadratic triangular B-spline, which next is expanded on calculation of the surface element for one triangle up to calculation of the whole 3D surface for fully triangulation. Consequently we propose an algorithm for generation of the knot net inside and on the boundary of the triangulation for purpose of calculation the whole quadratic triangular B-spline surface. Finally, we apply it to calculate the surface of the human head and present the results of the calculation as well as its textured avatar.

2 QUADRATIC TRIANGULAR B-SPLINE

While the constant triangular B-spline (TBS) is of zero order ($n = 0$) and the linear TBS of the first order ($n = 1$), the quadratic TBS is of the second order, when $n = 2$. It is calculated by three linear TBS according to the recurrent equation [7]. Let $V = \{\mathbf{t}_{00}, \mathbf{t}_{01}, \mathbf{t}_{02}, \mathbf{t}_{10}, \mathbf{t}_{20}\}$ be a group of points which determine a support of the quadratic TBS, as it is shown in Fig. 2a, where $\mathbf{t}_{00} = (h_{00}, v_{00})$, $\mathbf{t}_{10} = (h_{10}, v_{10})$, $\mathbf{t}_{20} = (h_{20}, v_{20})$ are vertices of the basic triangular and \mathbf{t}_{01} , \mathbf{t}_{02} are knots of the vertex \mathbf{t}_{00} . Then a recurrent equation for calculation of the quadratic TBS $M(\mathbf{u}|V)$ is as follows

$$M(\mathbf{u}|V) = \sum_i i = 0^2 \lambda_{ij}(\mathbf{u}|W) M(\mathbf{u}|V \setminus \{\mathbf{t}_{ij}\}) \quad (1)$$

where the sets $V \setminus \{\mathbf{t}_{ij}\}$, $j \in (0, 1, 2)$ are affinity independent quaternions of points selected from the set V by the manner of missing \mathbf{t}_{ij} , which determine the supports of corresponding linear TBS. After break down of eq. (1) for $j = 0$ we get

$$\begin{aligned} M(\mathbf{u}|\mathbf{t}_{00}, \mathbf{t}_{01}, \mathbf{t}_{02}, \mathbf{t}_{10}, \mathbf{t}_{20}) &= \lambda_{00}(\mathbf{u}) M(\mathbf{u}|\mathbf{t}_{01}, \mathbf{t}_{02}, \mathbf{t}_{10}, \mathbf{t}_{20}) \\ &+ \lambda_{10}(\mathbf{u}) M(\mathbf{u}|\mathbf{t}_{00}, \mathbf{t}_{02}, \mathbf{t}_{10}, \mathbf{t}_{20}) \\ &+ \lambda_{20}(\mathbf{u}) M(\mathbf{u}|\mathbf{t}_{00}, \mathbf{t}_{01}, \mathbf{t}_{02}, \mathbf{t}_{10}). \end{aligned} \quad (2)$$

From the previous equation it follows that the missed points have to create an affinity independent trinity $W = \{\mathbf{t}_{00}, \mathbf{t}_{10}, \mathbf{t}_{20}\}$ to which belongs the corresponding triplet of barycentric coordinates $\lambda_{00}(\mathbf{u})$, $\lambda_{10}(\mathbf{u})$, $\lambda_{20}(\mathbf{u})$. They are calculated as

$$\begin{aligned} \lambda_{00}(\mathbf{u}) &= \frac{d(\mathbf{u}, \mathbf{t}_{10}, \mathbf{t}_{20})}{d(\mathbf{t}_{00}, \mathbf{t}_{10}, \mathbf{t}_{20})}, \quad \lambda_{10}(\mathbf{u}) = \frac{d(\mathbf{t}_{00}, \mathbf{u}, \mathbf{t}_{20})}{d(\mathbf{t}_{00}, \mathbf{t}_{10}, \mathbf{t}_{20})}, \\ \lambda_{20}(\mathbf{u}) &= \frac{d(\mathbf{t}_{00}, \mathbf{t}_{10}, \mathbf{u})}{d(\mathbf{t}_{00}, \mathbf{t}_{10}, \mathbf{t}_{20})} \end{aligned} \quad (3)$$

* Laboratory of Digital Image Processing and Videocommunications, Department of Electronics and Multimedia Telecommunications, FEI TU Košice, Park Komenského 13, 041 20 Košice, Slovakia, jan.mihalik@tuke.sk

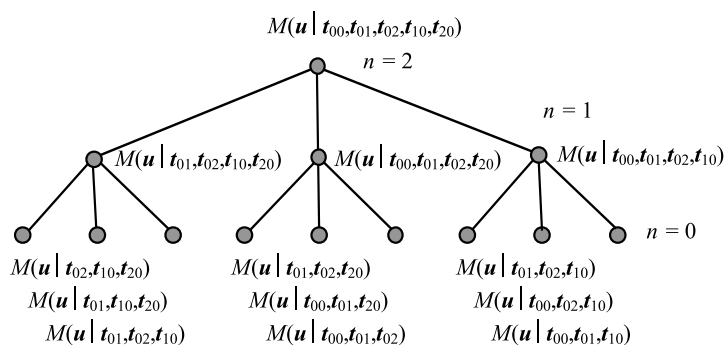


Fig. 1. Tree structure of the entire calculation the quadratic TBS $M(\mathbf{u}|t_{00}, t_{01}, t_{02}, t_{10}, t_{20})$

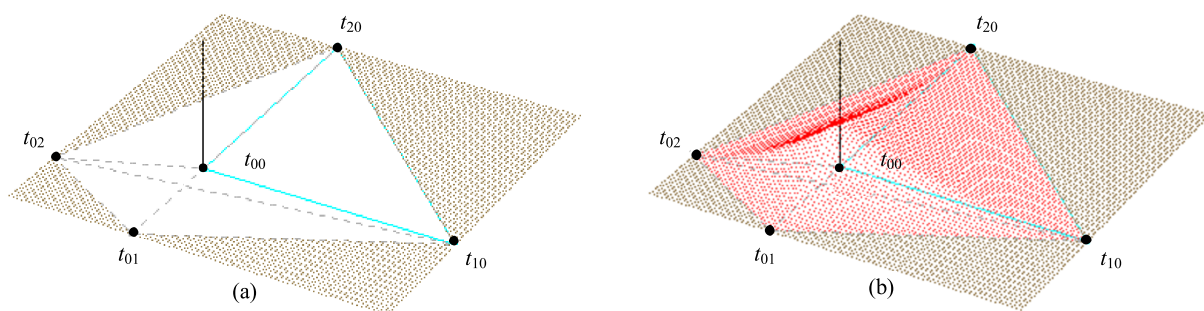


Fig. 2. a) Support, b) graph of quadratic TBS $M(\mathbf{u}|t_{00}, t_{01}, t_{02}, t_{10}, t_{20})$

where the determinants in denominators with the defined triplet of points are calculated as

$$|\det(V)| = d(\mathbf{t}_{00}, \mathbf{t}_{10}, \mathbf{t}_{20}) = \det \begin{pmatrix} 1 & 1 & 1 \\ h_{00} & h_{10} & h_{20} \\ v_{00} & v_{10} & v_{20} \end{pmatrix}. \quad (4)$$

In analogy, next determinants in nominators with different triples of points are calculated. For each point \mathbf{u} such values exist of the barycentric coordinates that it is valid

$$\mathbf{u} = \sum_{i=0}^2 \lambda_{i0}(\mathbf{u}) \mathbf{t}_{i0} \quad (5)$$

where $\sum_{i=0}^2 \lambda_{i0}(\mathbf{u}) = 1$. From the equation above it follows that they enable to localize the point \mathbf{u} in plane (h, v) only in regard to vertices $\mathbf{t}_{00}, \mathbf{t}_{10}, \mathbf{t}_{20}$ of the basic triangular, independently on its cartesian coordinate system.

At the same time the single linear TBS are calculated by a similar recurrent procedure, using three constant TBS with defined supports V (Fig. 1) and values

$$M(\mathbf{u}|V) = \begin{cases} \frac{1}{|\det(V)|} & \text{if } \mathbf{u} \in [V], \\ 0 & \text{if } \mathbf{u} \notin [V]. \end{cases} \quad (6)$$

Graphical presentation of the entire calculation of the quadratic TBS $M(\mathbf{u}|t_{00}, t_{01}, t_{02}, t_{10}, t_{20})$ by using the tree structure is in Fig. 1.

Then for the defined basic triangle, given by vertices $\mathbf{t}_{00}, \mathbf{t}_{10}, \mathbf{t}_{20}$, the face of resultant quadratic TBS will be dependent only on the position of knots as it is seen \mathbf{t}_{01} and \mathbf{t}_{02} from Fig. 2b.

Particular condition, necessary for correct calculation of the quadratic TBS, is the set of points of the linear TBS not to be collinear (do not lie on one line). If the condition is not met a contribution of the given linear TBS in the resultant quadratic TBS will be zero. Then negative values of the quadratic TBS occur in a part of its support. Assuming non-collinearity for them, the position of knots \mathbf{t}_{01} and \mathbf{t}_{02} is not limited, which means that they can be allocated anywhere in regard to the basic triangle (inside, outside, at vertices, on edges). We have two knots for each vertex of the basic triangle, i.e., \mathbf{t}_{01} and \mathbf{t}_{02} for vertex \mathbf{t}_{00} , next \mathbf{t}_{11} and \mathbf{t}_{12} for vertex \mathbf{t}_{10} and finally \mathbf{t}_{21} and \mathbf{t}_{22} for vertex \mathbf{t}_{20} . Afterward more quadratic TBS can be obtained for the same basic triangle. They will be calculated for supports, created always by the vertices of basic triangle and two different knots, i.e., $V = \{\mathbf{t}_{00}, \mathbf{t}_{01}, \mathbf{t}_{02}, \mathbf{t}_{10}, \mathbf{t}_{20}\}$, $\{\mathbf{t}_{00}, \mathbf{t}_{10}, \mathbf{t}_{11}, \mathbf{t}_{12}, \mathbf{t}_{20}\}$, $\{\mathbf{t}_{00}, \mathbf{t}_{10}, \mathbf{t}_{20}, \mathbf{t}_{21}, \mathbf{t}_{22}\}$, etc. Each set of the supports contains 5 points, from which 3 are the vertices of basic triangle. The procedure of calculation the quadratic TBS corresponding to separate supports is the same as for the one $V = \{\mathbf{t}_{00}, \mathbf{t}_{01}, \mathbf{t}_{02}, \mathbf{t}_{10}, \mathbf{t}_{20}\}$.

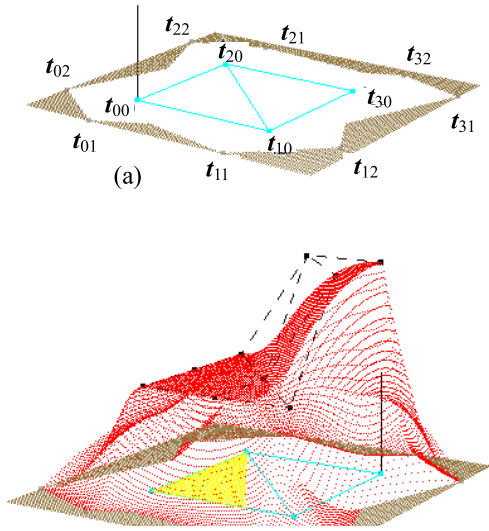


Fig. 3. a) Support, b) graph of the quadratic triangular B-spline surface over triangulation with two triangles

Table 1. Sets of points V_β^I and W_β^I with $|\beta| = \beta_0 + \beta_1 + \beta_2 = 2$

V_β^I	W_β^I	β_0	β_1	β_2
$V_{110}^I = \{t_{00}, t_{01}, t_{10}, t_{11}, t_{20}\}$	$W_{110}^I = \{t_{01}, t_{11}, t_{20}\}$	1	1	0
$V_{101}^I = \{t_{00}, t_{01}, t_{10}, t_{20}, t_{21}\}$	$W_{101}^I = \{t_{01}, t_{10}, t_{21}\}$	1	0	1
$V_{011}^I = \{t_{00}, t_{10}, t_{11}, t_{20}, t_{21}\}$	$W_{011}^I = \{t_{00}, t_{11}, t_{21}\}$	0	1	1
$V_{200}^I = \{t_{00}, t_{01}, t_{02}, t_{10}, t_{20}\}$	$W_{200}^I = \{t_{02}, t_{10}, t_{20}\}$	2	0	0
$V_{020}^I = \{t_{00}, t_{10}, t_{11}, t_{12}, t_{20}\}$	$W_{020}^I = \{t_{00}, t_{12}, t_{20}\}$	0	2	0
$V_{002}^I = \{t_{00}, t_{10}, t_{20}, t_{21}, t_{22}\}$	$W_{002}^I = \{t_{00}, t_{10}, t_{22}\}$	0	0	2

3 CALCULATION OF QUADRATIC TRIANGULAR B-SPLINE SURFACE

The quadratic triangular B-spline surface [8] is composed of the surface patches of separate triangles of the triangulation τ , which are calculated using TBS of the degree 2. Then points of the quadratic triangular B-spline patch for a triangle $I = \{t_{00}, t_{10}, t_{20}\}$ are calculated as follows

$$\begin{aligned} \mathbf{F}(\mathbf{u}) = & |\det(W_{110}^I)| M(\mathbf{u}|V_{110}^I) \mathbf{c}_{110}^I \\ & + |\det(W_{101}^I)| M(\mathbf{u}|V_{101}^I) \mathbf{c}_{101}^I + |\det(W_{011}^I)| M(\mathbf{u}|V_{011}^I) \mathbf{c}_{011}^I \\ & + |\det(W_{200}^I)| M(\mathbf{u}|V_{200}^I) \mathbf{c}_{200}^I + |\det(W_{020}^I)| M(\mathbf{u}|V_{020}^I) \mathbf{c}_{020}^I \\ & + |\det(W_{002}^I)| M(\mathbf{u}|V_{002}^I) \mathbf{c}_{002}^I \quad (7) \end{aligned}$$

where sets of points V_β^I determining the supports of separate quadratic TBS in eq. (7) and to them corresponding sets of points W_β^I for calculation of the normalization constants by their determinants with $\beta = \beta_0 + \beta_1 + \beta_2 = 2$ are in Tab. 1.

The number of the control points \mathbf{c}_β^I will be $\frac{(n+1)(n+2)}{2} = \frac{(2+1)(2+2)}{2} = 6$ out of which 3 after their orthographic

projection to the plane (h, v) are placed near the vertices of triangle I and the remaining 3 after the same projection near the centers of their sides.

The whole quadratic surface over the full triangulation τ is composed of the surface patches of separate triangles and can be calculated as [9]

$$\mathbf{P}(\mathbf{u}) = \sum_{I \in \tau} \sum_{|\beta|=n} |\det(W_\beta^I)| M(\mathbf{u}|V_\beta^I) \mathbf{c}_\beta^I. \quad (8)$$

In general, modeling of the quadratic triangle B-spline surface can be carried out by changing the position of control points \mathbf{c}_β^I as well as distribution of knots. Allocation of knots for separate vertices of the triangulation τ will affect its smoothness. Note, that nonzero contributions of the particular surface patches are not only in areas of corresponding triangles, but also in surrounding outside of them determined by supports of their quadratic triangular B-splines $M(\mathbf{u}|V_\beta^I)$ in eq. (8). This is a basic difference from the classical methods of construction of surfaces, for example by using Bézier's surface patches [10]. Just interference of the quadratic triangular B-spline surface patches ensures a global smoothness of the whole surface without additional limitations of positions of control points.

For the assumed triangulation τ in Fig. 3a, composed of two triangles with one adjoining side or two common vertices, the number of knots is 8 and control points 9. To the vertices belong not only to the same knots but the control points, too. In addition, the next two control points belong to the center of the adjoining side. Possible forms of the modeled quadratic triangular B-spline surface, for the triangulation in Fig. 3a, along with control nets are shown in Fig. 3b.

4 GENERATION OF KNOT NET

The designed algorithm of generation of the knot net follows from the univariant Monte Carlo method [11]. This method has one level of variance, namely the distances of the knots from a vertex to which the knots are assigned. This algorithm is useful for symmetric objects like the human head where in an ideal case left and right half are equal.

4.1 Generation of knots for vertices inside the triangulation

In this case, the vertex t_{i0} for which two knots will be generated do not lie on the boundary of triangulation. Then we have to find all triangles that have the vertex t_{i0} in common as can be seen in Fig. 4a. Consequently, we will determine two lines p_1 and p_2 crossing through the vertex t_{i0} and are axes of the biggest angle α_1 and the second biggest one α_2 of these triangles (Fig. 4b). Next, the distance D_1 is defined as approximately one third of the length of shorter side d_1 of the triangle with the

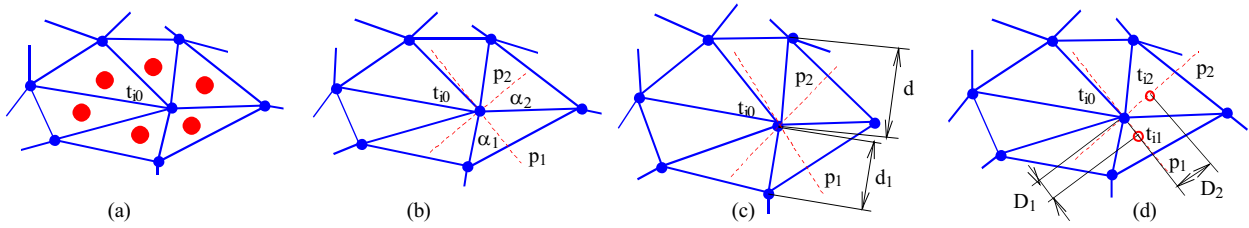


Fig. 4. Generation of two knots for the vertex t_{i0} inside the triangulation

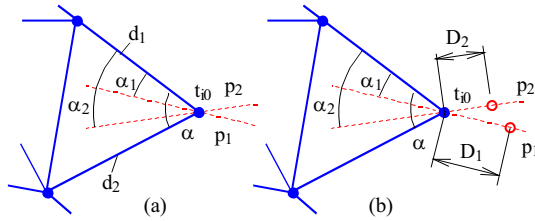


Fig. 5. Generation of two knots for the vertex t_{i0} of one triangle on the boundary of triangulation

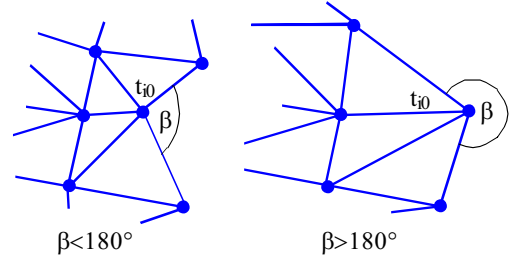


Fig. 6. Possible angles between marginal sides of triangles

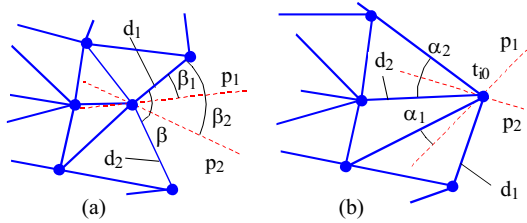


Fig. 7. Manners of division of outer angle a) $\beta < 180^\circ$, b) $\beta > 180^\circ$

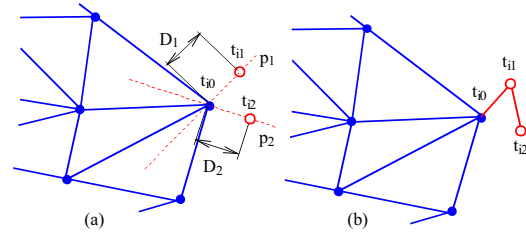


Fig. 8. a) Allocation of the knots t_{i1} and t_{i2} for $\beta > 180^\circ$, b) their symbolic representation

biggest angle and with the vertex t_{i0} and the distances D_2 – as approximately one third of the length of shorter side d_2 of the triangle with the second biggest angle and with the same vertex t_{i0} (Fig. 4c). Then we allocate the knot t_{i1} on the line p_1 in distance D_1 and similarly t_{i2} on the line p_2 in distance D_2 from the vertex t_{i0} in direction inside of the corresponding triangle (Fig. 4d).

Finally, we will check whether all conditions for allocation of the knots are fulfilled [3]. If not so we systematically reduce the distances in case that the knots interfere with triangles, which do not have the vertex t_{i0} . Also we change a slope of the line p_1 or p_2 , when the knots lie collinearly with some vertex or one of them lies on a line determined by a side of one of the triangles.

4.2 Generation of knots for vertices on the boundary of triangulation

In case that we have just one triangle with the vertex t_{i0} on the boundary of triangulation, we will follow such a way. Two lines p_1 and p_2 are determined crossing through the vertex t_{i0} and dividing inner angle α of the triangle at the vertex t_{i0} into $\alpha_1 = (1/3)\alpha$ and $\alpha_2 = (2/3)\alpha$ (Fig. 5a). Then the distances D_1 and D_2

are defined as approximately one third of the length of corresponding sides d_1 and d_2 of the triangle with the vertex t_{i0} closer to the line p_1 and p_2 , respectively as can be seen in the same Fig. 5a. Afterwards, we will allocate the knots t_{i1} and t_{i2} on the lines p_1 and p_2 in distances D_1 and D_2 from the vertex t_{i0} , respectively in direction out of the corresponding triangle or out of the triangulation (Fig. 5b).

If there are more triangles with the vertex t_{i0} on the boundary of triangulation, so at first we will define outer angle β that is contained by marginal sides of the triangles where t_{i0} is one of their vertices (Fig. 6).

When outer angle $\beta < 180^\circ$, then we will determine two lines p_1 and p_2 crossing through the vertex t_{i0} and dividing outer angle β into $\beta_1 = (1/3)\beta$ and $\beta_2 = (2/3)\beta$ (Fig. 7a). Consequently, the distances D_1 and D_2 are defined as approximately one third of the length of sides d_1 and d_2 of the triangles with the vertex t_{i0} closer to the line p_1 and p_2 , respectively as can be seen in the same Fig. 7a. Similarly we proceed if outer angle $\beta > 180^\circ$. Then we will determine two lines p_1 and p_2 crossing through the vertex t_{i0} which are axes of the biggest angle α_1 and the second biggest one α_2 , respectively from all triangles with this vertex (Fig. 7b). Also for these lines

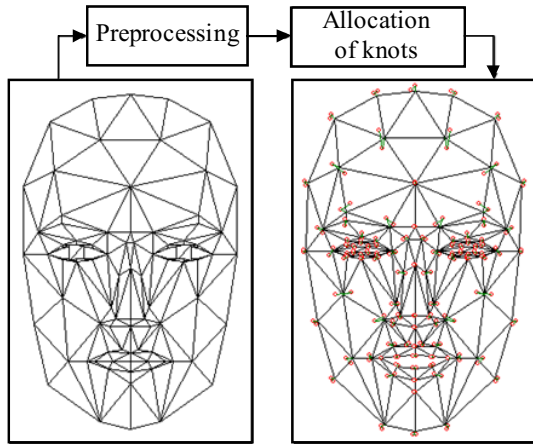


Fig. 9. a) Orthographic projection of the model Candide. b) Generated knot net for the triangulation τ of the model

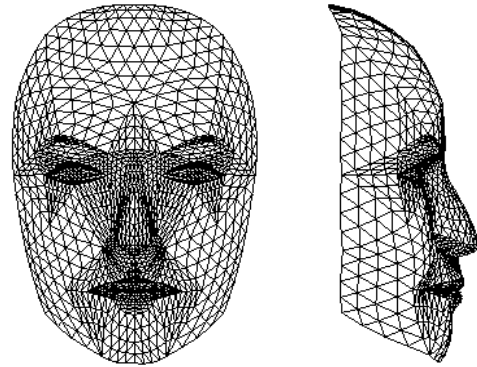


Fig. 10. The quadratic triangular B-spline surface of human head

5 EXPERIMENTAL RESULTS

The proposed algorithm for generation of knot net was applied on calculation of the quadratic triangular B-spline surface of the human head [3]. It is based on its 3D polygonal model which is determined by a list of vertices and polygons. Vertices are defined by their coordinates in R^3 and polygons-by the ones that create them. Typical polygons are triangles or quadrangles. The main advantage of triangles is, that their vertices always lie in the same plane what leads to simple manipulation with them such as in graphical means of OpenGL. A density of polygons in 3D model of the human head depends on a number of details of its separate parts like eyes, mouth, nose, *etc.* For our purposes we used free available 3D polygonal model Candide 3-1-6 [12], which contains 113 vertices and 184 polygons (triangles) and represents a course approximation of the surface of human head.

The triangulation τ , over which the quadratic triangular B-spline surface of the human head will be calculated is given by the orthographic projection of the model Candide from R^3 to the plane of coordinates (h, v) , *ie* by its front view in Fig. 9a. Then two knots are allocated to each of its vertices such a way to be valid the condition of normality over the full triangulation τ . However, for them some non accepted positions have to be excluded [3]. In preprocessing of the input triangulation τ there are established the limitations for positions of knots and then their assigning to separate vertices is carried out by the proposed algorithm. The result of generation the knot net for the triangulation τ by the algorithm is illustrated in Fig. 9b. The knots have an influence on the calculated quadratic triangular B-spline surface of the human head in area of intersection of supports of the separate quadratic TBS with vertices to which the ones are assigned. The biggest influence of the knots on the surface is near of their surroundings.

Provided that the allocation of knots is correct, when the condition of normality is valid over the full triangulation τ next modeling of the surface of human head is pos-

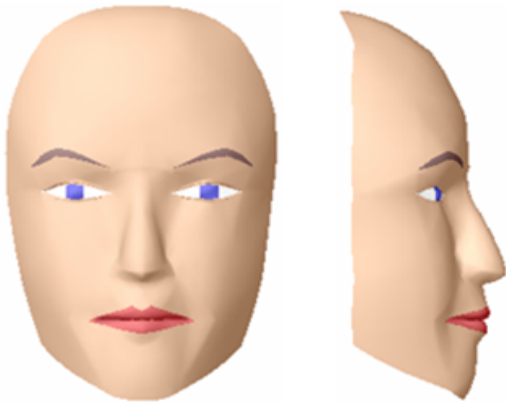


Fig. 11. The modeled human head of a selected avatar by the quadratic triangular B-spline surface

we will define the distance D_1 as approximately one third of the length of shorter side d_1 of the triangle with the biggest angle α_1 and the distance D_2 – of the length of shorter side d_2 of the triangle with the second biggest angle α_2 and with the common vertex t_{i0} (Fig. 7b).

Afterwards, we will allocate the knots t_{i1} and t_{i2} on the lines p_1 or p_2 in distance D_1 and D_2 , respectively from the vertex t_{i0} in direction out of the corresponding triangle. These are shown for $\beta > 180^\circ$ in Fig. 8a together with their symbolic representation in Fig. 8b, where t_{i0} is connected with the knot t_{i1} and that one is connected with t_{i2} . This symbolic representation just simplifies their imaging in the full triangulation. Similarly, the knots for $\beta < 180^\circ$ would be allocated including their symbolic representation, which can be generalized also for vertices inside the triangulation. Finally, we will check whether all conditions for allocation of the knots on the boundary are fulfilled, similarly as it was inside the triangulation, including their possible correction.

sible by control points \mathbf{c}_β^I in space R_3 with coordinates (h, v, r) [3]. The surface of human head can be calculated continually in each point inside the input triangulation or over its finer structure that we used on calculation of the resultant surface in Fig. 10. After its texturing by texture of a selected avatar the modeled human head is in Fig. 11.

6 CONCLUSION

The quadratic triangle B-spline surface of the human head is smooth also for a wireframe (edginess) 3D model. The surface is created by surface patches calculated using the quadratic triangular B-splines for separate triangles of the orthographical projection of the 3D model. The shape of the surface is given by the distribution of control points and its smoothness is affected by knot net. Relationship between the surface and knot net is invariant toward transformations like scaling, rotation and translation. The proposed algorithm of generation the knot net is universal and can be applied to calculate the quadratic triangle B-spline surface of any 3D object.

MPEG-4 SNHC specifies for 3D polygonal models of the human head their neutral (initial) state as well as feature points. These are arranged in groups referring to certain parts of the human head as mouth, nose, eyes, etc. By using the feature points from the real human head it is possible to form a selected universal polygonal 3D model in such a way that its feature points are in coincidence with those from the real human head. Coordinates of the feature points of the real human head represent facial definition parameters (FDP) and in the simplest case they can be directly obtained from the output of 3D scanner. Then on the basis of knowledge FDP, using the proposed algorithm for generation of knot net, it is possible to create the quadratic triangular B-spline surface with the shape of a real human head which is very important part of its cloning [13].

Recently, information and communication technologies are extended from the real environment to virtual one [14]. In these environments, an important object is human who can be represented in their interiors as avatar (virtual) or clone. In general, inside of the interiors may occur avatars and clones together. The dialog between them is carried out by using their cloned or virtual heads. Then virtual videocommunication enables far-distant participants to see the dialog inside the same virtual environment in which they are indirectly presented.

REFERENCES

- [1] The Special Issue of the IEEE Trans. on Circuits and Systems for Video Technology on MPEG-4 SNHC, July 2004.
- [2] MIHALÍK, J.: Standard Videocodec MPEG-4, *Electronic Horizon* **60** No. 2 (2003), 7–11. (In Slovak)
- [3] MIHALÍK, J.: Modeling of Human Head Surface by using Triangular B-Splines., *Radioengineering*, **19**, No. 1, 2010, p.39-45.
- [4] MIHALÍK, J.—MICHALČIN, V.: Animation of 3D Model of Human Head, *Radioengineering* **16** No. 1 (2007), 58–66.
- [5] MIHALÍK, J.—MICHALČIN, V.: Texturing of Surface of 3D Human Head Model, *Radioengineering* **13** No. 4 (2004), 44–47.
- [6] STRINTZIS, M.—SARRIS, N. Eds.: 3D Modeling and Animation: Synthesis and Analysis Techniques for the Human Body, IRM Press, Hershey, PA, July 2004.
- [7] GREINER, G.—SEIDEL, H. P.: Modeling with Triangular B-Splines, *IEEE Computer Graphics and Applications*, **14** (1994), 56–60.
- [8] ROSSE, C.—ZEILFELDER, F.—NUMBERGER, G.—SIEDEL, H. P.: Reconstruction of Volume Data with Quadratic Super Splines, *Trans. on Visualization and Computer Graphics* (2004), 38–42.
- [9] FONG, P.—SEIDEL, H. P.: An Implementation of Triangular B-Spline Surfaces over Arbitrary Triangulations, *Computer Aided Geometric Design* **25** No. 10 (1993), 265–267.
- [10] PRAUTZSCH, H.—BOEHM, W.—PALUSZNY, M.: Bézier and B-Spline Techniques, Springer Verlag, 2002.
- [11] DAHMEN, W.—MICCHELLI, C. A.: Multivariate Splines - a New Constructive Approach. *Surfaces in Computer Aided Geometric Design*, North-Holland, Amsterdam, 1992, pp. 191–215.
- [12] AHLBERG, J.: Candide-3: An Updated Parameterised Face, Rep.No. LiTH-ISY-R-2326, Jan 2001.
- [13] PIEGL, L.—TILLER, W.: Parametrization for Surface Fitting in Reverse Engineering, *Computer Aided Geometric Design* **33** No. 11 (2001), 593–603.
- [14] JOSLIN, CH.—PANDZIC, I, S.—THALMANN, N. M.: Trends in Networked Collaborative Virtual Environments, *Computer Communications* **26** No. 5 (2003), 430-437.

Received 16 October 2010

Ján MIHALÍK graduated from Technical University in Bratislava in 1976. Since 1979 he joined Faculty of Electrical Engineering and Informatics of Technical University of Košice, where received his PhD degree in Radioelectronics in 1985. Currently, he is Full Professor of Electronics and Telecommunications and the head of the Laboratory of Digital Image Processing and Videocommunications at the Department of Electronics and Multimedia Telecommunications. His research interests include information theory, image and video coding, digital image and video processing and multimedia videocommunications.